Langmuir
Article
pubs.acs.org/Langmuir

Tethering Hydrophobic Peptides to Functionalized Self-Assembled Monolayers on Gold through Two Chemical Linkers Using the Huisgen Cycloaddition

Ignacio F. Gallardo and Lauren J. Webb*

Department of Chemistry and Biochemistry, Center for Nano- and Molecular Science and Technology, and Institute for Cell and Molecular Biology, 1 University Station A5300, The University of Texas at Austin, Austin, Texas 78712, United States

Received September 12, 2010. Revised Manuscript Received November 2, 2010

Gold surfaces functionalized with an α-helical peptide have been generated by reacting an azide-terminated self-assembled monolayer with structured peptides containing two cyanophenylalanines through a Huisgen cycloaddition. Mixed monolayers of a reactive bromine-terminated thiol and inert alkane thiol were prepared at various concentrations of the Br-terminated moiety. These were reacted with sodium azide to form azide-terminated monolayers with controlled concentration of the reactive azide. These surfaces were studied through ellipsometry and X-ray photoelectron spectroscopy, which demonstrated that the concentration of the reactive azide group on the surface is controlled by the chemical conditions under which the monolayer is prepared. Grazing incident angle surface infrared spectroscopy (GRAS-IR) of the azide-terminated surface demonstrated that the azide is approximately perpendicular to the plane of the surface, as expected. These surfaces were then exposed to an α-helical peptide composed of alternating leucine and lysine residues, with two residues replaced with cyanophenylalanine to react with two neighboring surface-bound azide groups to bind the peptide to the surface through two covalent bonds. The yield of this reaction was quantified through monitoring the absorption of the azide group by GRAS-IR. Despite damage to the monolayer during the reaction, reaction yields of 80−98% were determined for optimized reaction conditions. Although the peptide retains its α-helical configuration under the reaction conditions, GRAS-IR analysis of the amide I and II modes of the surface-bound peptide showed that it is probably randomly oriented on the surface.

Introduction

Proteins possess a tremendous range of biological function that cannot currently be artificially reproduced with modern device fabrication or chemical synthesis, such as ligand binding (sensing) and reactivity (catalysis). Incorporation of these functions into engineered devices through the integration of biological molecules with inorganic substrates and materials is an area of active research, with applications as diverse as sensing, molecular electronics, biofuels, electrochemistry, proteomics, and beyond.[1,2] This goal requires an intimate, controlled, and reproducible contact between the biological and inorganic materials. Successful sensing devices based on surface-bound antibody and RNA aptamer sensors have been demonstrated,[3,4] but incorporation of the biological function of proteins onto surfaces has been slower.[5,6] Uncontrolled absorption of a protein on an ill-defined surface is relatively easy to achieve,[7,8] but this often results in loss of the desired protein function because of unfolding, aggregation, improper orientation, or other factors.[9] Furthermore, without adequate surface characterization, reproducibility and control are difficult to achieve.[10]

To this end, there is currently great interest in placing proteins onto inorganic surfaces reliably, and a number of creative methods have been devised such as surface functionalization with biologically compatible polymers,[11−13] surface substrate attachment,[6,14] affinity tagging with reagents such as biotin/avidin or hexa-histidine affinity to Ni(II)-nitrilotriacetic acid (Ni-NTA),[15−17] and covalent bonding through surface amino acid side chains.[6,18] Several supported lipid bilayer architectures have been shown to be capable of surface-attachment of membrane-bound and membrane-associated proteins, but this technology is of course confined to this class of proteins.[19−21] A central limitation of many of these strategies is that they result in a substrate that is covered with an inert blocking layer that can be significantly larger in dimension

*To whom correspondence should be addressed. E-mail: lwebb@cm.utexas.edu.

(1) Barton, S. C.; Gallaway, J.; Atanassov, P. *Chem. Rev.* **2004**, *104*, 4867–4886.
(2) Gianese, G.; Rosato, V.; Cleri, F.; Celino, M.; Moreales, P. *J. Phys. Chem. B* **2009**, *113*, 12105–12112.
(3) Ligler, F. S. *Anal. Chem.* **2009**, *81*, 519–526.
(4) Taitt, C. R.; Shriver-Lake, L. C.; Ngundi, M. M.; Ligler, F. S. *Sensors* **2008**, *8*, 8361–8377.
(5) Kulagina, N. V.; Lassman, M. E.; Ligler, F. S.; Taitt, C. R. *Anal. Chem.* **2005**, *77*, 6504–6508.
(6) Willner, I.; Katz, E. *Angew. Chem., Int. Ed.* **2000**, *39*, 1180–1218.
(7) Halthur, T. J.; Arnebrant, T.; Macakova, L.; Feiler, A. *Langmuir* **2010**, *26*, 4901–4908.
(8) Williams, R. A.; Blanch, H. W. *Biosens. Bioelectron.* **1994**, *9*, 159–167.
(9) Langer, R.; Tirrell, D. A. *Nature* **2004**, *428*, 487–492.
(10) North, S. H.; Lock, E. H.; King, T. R.; Franek, J. B.; Walton, S. G.; Taitt, C. R. *Anal. Chem.* **2010**, *82*, 406–412.
(11) Haab, B. B.; Dunham, M. J.; Brown, P. O. *Genome Biol.* **2001**, *2*, 1–13.
(12) Leung, B. O.; Wang, J.; Brash, J. L.; Hitchcock, A. P. *Langmuir* **2009**, *25*, 13332–13335.
(13) Zheng, H.; Du, X. *J. Phys. Chem. B* **2009**, *113*, 11330–11337.
(14) Blanford, C. F.; Heath, R. S.; Armstrong, F. A. *Chem. Commun.* **2007**, 1710–1712.
(15) Bader, G. D.; Donaldson, I.; Wolting, C.; Ouellette, B. F. F.; Pawson, T.; Hogue, C. W. V. *Nucleic Acids Res.* **2001**, *29*, 242–245.
(16) Chevalier, S.; Cuestas-Ayllon, C.; Grazu, V.; Luna, M.; Feracci, H.; De la Fuente, J. M. *Langmuir* **2010**, *26*, 14707–14715.
(17) Lapin, N. A.; Chabal, Y. J. *J. Phys. Chem. B* **2009**, *113*, 8776–8783.
(18) Millo, D.; Pandelia, M. E.; Utesch, T.; Wisitruangsakul, N.; Mroginski, M. A.; Lubitz, W.; Hildebrandt, P.; Zebger, I. *J. Phys. Chem. B* **2009**, *113*, 15344–15351.
(19) Du, X.; Wang, Y. *J. Phys. Chem. B* **2007**, *111*, 2347–2356.
(20) Ganesan, P. V.; Boxer, S. G. *Proc. Natl. Acad. Sci. U.S.A.* **2009**, *106*, 5627–5632.
(21) Tsujiuchi, Y.; Furuya, K.; Matsumoto, J.; Makino, Y.; Ito, M.; Masumoto, H.; Goto, T. *Thin Solid Films* **2009**, *518*, 600–605.

than the protein itself, resulting in a surface that is dominated by the chemical properties of the blocking layer and that has limited or nonexistent capability to control the orientation of the surface-associated protein.

A significant impediment to the advancement of this goal is the general observation that proteins tend to lose function as a consequence of placing a soft, solution-phase material in the perturbed chemical, structural, and electrostatic environment that occurs on and near surfaces. One approach to this problem is to fabricate chemically functionalized surfaces that mimic biologically relevant protein−protein assembly conditions. In the complex milieu of a living cell, proteins assemble into robust and functional structures by relying almost exclusively on noncovalent interaction mechanisms directed by the presence of strong, localized electrostatic fields on the protein surface. Fabricating chemically functionalized surfaces that accurately mimic a stable and functional biological interface could create an environment that replicates and controls the interactions between proteins on a wholly artificial substrate. To this end, we are using surface functionalization chemistry to tether carefully selected peptides to a surface in a structurally controlled manner. Here, the functionalization chemistry that binds a protein to a surface is carefully controlled through the chemical functionalization method chosen, is relatively thin, and directs the extent and structure of all subsequent surface chemistry. The surface-bound peptide then interacts with and selectivity binds proteins introduced from solution based on the localized and directional electrostatic forces that dominate biomolecular interactions in the living cell.

In this Article, we present the necessary first step to achieve this goal: surface functionalization of carefully selected peptides to a well-characterized surface. Here we present our surface functionalization strategy for preparing reactive self-assembled monolayers (SAMs) on gold surfaces,[22,23] resulting in an azide (N_3)-terminated surface. This surface is then exposed to an α-helical peptide containing two nitrile functional groups a known distance apart, and through a Huisgen cycloaddition ("click") reaction, results in a peptide that is chemically tethered to the surface at two points. Each prepared surface is characterized with X-ray photoelectron spectroscopy (XPS), ellipsometry, and grazing incidence angle reflection−absorption infrared spectroscopy (GRAS-IR) to determine the chemical composition of the resulting surface. The extent of the surface functionalization reaction is determined through GRAS-IR measurements by monitoring the disappearance of the azide signal, which quantizes the extent of the reaction, and appearance of amide peaks, which can determine the physical orientation of the peptide with respect to the surface normal. We present initial data on controlling the surface structure of chemically bound peptides through careful choice of reaction conditions, a necessary first step in using peptides as a chemical recognition element of protein−surface interactions.

Materials and Methods

A. Preparation of Peptides. The peptide GGPGXLKK-LLKKLLKKLLKKLXGGPG (called αKL(CN-Phe)), where X = *p*-cyanophenylalanine (CN-Phe), was prepared using standard Fmoc solid state peptide synthesis. Fmoc-*p*-cyanophenylalanine was obtained from PepTech Corp. (Burlington, MA). The final mass of the purified product, 2823.32 Da, was confirmed with an ABI Voyager MALDI-TOF mass spectrometer with α-cyano-4-hydroxycinnamic acid as the matrix.

B. Circular Dichroism Spectroscopy. Solutions of 100 μM αKL(CN-Phe) peptide were prepared in a buffer composed of 50 mM Tris pH = 7.5, 100 mM NaCl, in a solution of 5% (v/v) water in tetrahydrofuran (THF). Circular dichroism (CD) spectroscopy was performed on a Jasco J-815 CD spectrometer illuminating between 190−250 nm.

C. Surface Functionalization. Substrates were fabricated on 500 μm thick silicon (111) wafers (University Wafer) polished on one side and sealed in N_2(g). The sealed wafer package was opened in a dry N_2(g) atmosphere inside a glovebox and transferred inside sealed containers to a Class 100/1000 clean room. Wafers were exposed to a stream of ultrapure N_2(g) and used without further cleaning. The surfaces were covered in 10 nm of chromium followed by 100 nm of gold (99.95% pure) using a Thermal Evaporator-II (Denton) instrument at a pressure of 10^{-5} Torr. After Au deposition, the wafers were covered with clean-room rated silicon wafer tape (ICROS TAPE) and cut with a programmable Disco 321 wafer dicing saw into pieces approximately 4 cm^2 if intended for infrared spectroscopy or approximately 1 cm^2 for all other measurements. A series of 5× to 100× inspections with an optical microscope (Probe Station-I and Analyzer Karl Suss PM 5) confirmed that use of the wafer tape during dicing considerably reduced the number of residual Si crystals on top of the Au. After the tape was removed from each individual sample, the clean substrates were sonicated for 10 min in acetone to remove any tape residue. The surfaces were then cleaned by immersion for 2 min in piranha solution (1:3 30% hydrogen peroxide/concentrated sulfuric acid; ***caution****: explosive in the presence of organic contaminants*) and rinsed sequentially in ultrapure water with an impedance of >18 MΩ/cm (Barnstead NANOpure Diamond Life Science UV/UF), hydrochloric acid, water, and anhydrous ethanol. After the last ethanol rinsing, samples were completely dried under a stream of N_2(g).

The SAM solution was made with the desired thiol diluted in anhydrous ethanol. 11-Bromo-1-undecanethiol (BrUDT, 99% purity in a 1 mM solution in ethanol, Asemblon, Redmond, WA), was mixed with decanethiol (DT, 96%, Sigma Aldrich) to different concentrations, keeping the total thiol concentration constant at 1 mM. Surfaces were functionalized in solutions in which the concentration of BrUDT was 0, 20, 25, 50, 75, and 100% of the total thiol concentration; we report the composition of the monolayer based on the percentage of reactive BrUDT in this initial solution. The substrates were immersed in this solution for 24 h to ensure highly packed thiol surfaces.[24] The samples were then removed, rinsed in water followed by anhydrous ethanol, and dried under a stream of N_2(g).

The Br-terminated SAMs were immersed in 8 mL of a solution of saturated sodium azide (NaN_3, Sigma Aldirch) in dimethylformamide (DMF) for 48 h in the dark. They were then removed and rinsed sequentially with water, anhydrous ethanol, acetone, toluene, acetone, and anhydrous ethanol. The surfaces were then sonicated for 5 min in ethanol and dried under a stream of N_2(g). Care was taken at all times to handle and store SAM-covered surfaces in the dark to avoid light exposure.

To react the azide-terminated surface with a nitrile-containing peptide through a Huisgen cycloaddition, N_3-terminated SAMs were immersed in 15 mL of THF with 300 nmol of peptide and 50 mol equiv of diethyl azodicarboxylate (DEAD, 40 wt % in toluene, Sigma Aldirch). In some cases, to improve solubility, peptides were dissolved in 1 mL of water and then diluted with 14 mL of THF. The peptide solution was stirred for 24 h at room temperature in the dark in sample holders that had been purged under a N_2(g) flow. The sample was situated such as to avoid damage from the stir bar. After 24 h, substrates were rinsed in 37 °C water followed by ethanol and dried under a stream of N_2(g). Dried samples were stored in the dark.

D. Ellipsometry. The thickness of the SAMs was determined with a J.A. Woollam M2000 spectroscopic ellipsometer illuminating

(22) Tam-Chang, S. W.; Biebuyck, H. A.; Whitesides, G. M.; Jeon, N.; Nuzzo, R. G. *Langmuir* **1995**, *11*, 4371–4382.
(23) Nuzzo, R. G.; Allara, D. L. *J. Am. Chem. Soc.* **1983**, *105*, 4481–4483.
(24) Collman, J. P.; Devaraj, N. K.; Chidsey, C. E. D. *Langmuir* **2004**, *20*, 1051–1053.

with broad-spectrum radiation at incident angles of 70° and 75° with respect to the surface normal. To determine the thickness (t) of the surface monolayer, only reflections detected at energies between 300 and 600 nm were used. The data were fit to a model consisting of a Si substrate with a layer of Cr 10 nm thick, and a layer of Au 100 nm thick, both of which were fixed. The optical constants for the SAM layer were taken from those of C_2H_4 with an initial thickness of 6 nm.[25] The model was not affected by changes in the initial thickness conditions if such changes were less than a few nanometers and as long as the initial condition was larger than the output of the model. The thickness of the monolayer on a given sample was determined from the average of five measurements on different parts of that sample. We report the average of three such samples to determine the thickness of each chemically functionalized surface.

E. X-ray Photoelectron Spectroscopy. X-ray photoelectron spectroscopy of all surfaces was conducted on a Kratos Azis Ultra XPS with a monochromatic Al Kα X-ray source illuminating at 1486.5 eV. The ultrahigh vacuum (UHV) chamber was kept below pressures of 2×10^{-9} Torr during sample measurement. Samples were illuminated with a spot $300 \times 700\,\mu m^2$ in dimension. Survey spectra were collected from 0 to 1000 eV with a resolution of 1 eV, while high resolution spectra were collected with a pass energy of 20 eV and a resolution of 0.1 eV. All measurements were obtained with the hemispherical electron energy analyzer positioned normal to the sample surface unless explicitly indicated. To increase the resolution of detailed scans of Br-terminated surfaces, data were occasionally collected with the detector positioned at an angle of 42° with respect to the surface normal, to reduce the background signal from Au.

To quantify the surface composition of detected atoms, the Kratos XPS software was used to determine the integrated area (I_x) under all photoelectron peaks of interest.[26] Baselines of the S and N, and Na peaks were fit to a linear function and baselines for Au, C, O, and Br were fit to a Shirley baseline function.[27,28] These measured areas were then scaled by the sensitivity factors (S_x) of each peak (6.25, 0.278, 0.668, 1.055, 0.78, and 1.685 for the Au 4f, C 1s, S 2p, Br 3d, O 1s, and N 1s peaks, respectively) to compute the atom fraction (C_x) for each element according to eq 1:

$$C_x = \frac{I_x/S_x}{\sum_i I_i/S_i} \quad (1)$$

This was multiplied by 100 to determine the surface atom percentage of each element in our measurement.

F. GRAS-IR. Surface vibrational spectroscopy was collected with a Bruker Vertex 70 Fourier transform infrared (FTIR) spectrometer equipped with a A518/Q Horizontal Reflection (Bruker) instrument for illuminating the sample at a grazing angle of 80° with respect to the surface normal. The sample chamber was continuously purged with N_2(g), and once inside the chamber samples were transferred with a home-built externally controlled sample manipulation arm to avoid breaking the N_2(g) purge. The chamber was continuously purged for 1 h before any measurements to reduce background noise from H_2O and CO_2. All measurements were made with p-polarized light. Two sets of scans were collected for each sample. For the first, a mercury cadmium telluride (MCT) detector was used to collect 100 scans between 400 and 4000 cm^{-1} at a resolution of 4 cm^{-1}, ideal for the amide carbonyl peaks between 1500 and 1700 cm^{-1}. For the second, an indium antimonide (InSb) detector was used to collect 100 scans between 1870 and 4000 cm^{-1} at a resolution of 4 cm^{-1} to take advantage of its superior sensitivity for the N_3 absorption near 2100 cm^{-1}. All samples were referenced to a common clean bare gold substrate to compare absolute differences of all observed signals between different samples. After background subtraction, the baseline of each spectrum was flattened with a linear polynomial function, and the integral under the peak of interest was then computed with the FTIR instrument's OPUS software.

To determine the extent, if any, of the degradation of the azide peak under these reaction conditions that was not associated with the cycloaddition reaction, N_3-terminated surfaces were exposed to all reaction and rinsing conditions in the absence of peptide, and the azide peak was measured by GRAS-IR. To determine the extent of peptide physisorption to the surface in the absence of the cycloaddition reaction, a SAM composed only of DT (i.e., containing no reactive azide functionality) was exposed to the peptide-containing reaction solution and then rinsed and dried as normal. The amide region of this sample was measured by GRAS-IR to determine the presence of physisorbed peptide.

Table 1. Thickness (t) of SAMs Measured by Ellipsometry[a]

percentage of Br in SAM	t [nm]
Au substrate	0.4 ± 0.1
0% Br	1.5 ± 0.2
25% Br	1.5 ± 0.2
50% Br	1.6 ± 0.2
75% Br	2.0 ± 0.2
100% Br	2.0 ± 0.2
dodecanethiol	2.0 ± 0.1
hexadecanethiol	2.4 ± 0.1

[a] SAMs composed of mixed monolayers of 11-Br-1-undecanethiol and decanethiol are shown as a function of the percentage of the Br-terminated thiol in the reaction solution; dodecanethiol; and hexadecanethiol. The thickness of the monolayer on a single sample was determined from the average of five measurements on different locations on the sample. We report the average and one standard deviation from three such samples.

Results

A. Br- and N_3-Terminated Surfaces. Ellipsometry was used to estimate the thickness of each Br- and N_3-terminated monolayer, and the results are summarized in Table 1.[29] In this measurement, the average thickness of each monolayer is a function of the length of the thiol alkyl group and the percentage of Br-terminated thiols present in the mixed monolayer. On a bare, clean Au substrate, we measured a surface coverage thickness of 0.4 ± 0.1 nm, indicating that an adventitious carbon layer formed in the 5 min that it took to clean the samples and perform the ellipsometery measurement. There is a positive correlation between the thickness of the SAM and the average thiol length used to form it. The 0% BrUDT (i.e., 100% DT) sample had a thickness of 1.5 ± 0.2 nm, and the 100% BrUDT SAM had a thickness of 2.0 ± 0.2 nm. Mixed monolayers made with increasing concentrations of BrUDT resulted in surface thicknesses between these two extremes. Furthermore, the surface composed of 100% BrUDT showed the same thickness as a surface composed of 100% dodecane thiol SAM. Because of the large size of the terminating Br atom on BrUDT, the difference between these two thiols is a single Br atom versus a CH_3 which differs in classical atomic diameter by less than 0.07 nm,[30] less than the averaged SAM thickness error. One of the sources for this error, in the case of the BrUDT-terminated SAMs, was most likely the optical constants used in the model. The complex index of refraction that was used to fit the ellipsometry data for the SAM was that of a layer of C_2H_4, and thus did not take into

(25) Palik, E. *Handbook of Optical Constants of Solids II*; Academic Press: Orlando, FL, 1998.
(26) Moulder, J. F.; Stickle, W. F.; Sobol, P. E.; Bomben, K. D. *Handbook of X-ray Photoelectron Spectroscopy*; Physical Electronics, Inc.: Eden Prairie, MN, 1995.
(27) Kankate, L.; Turchanin, A.; Goelzhaeuser, A. *Langmuir* **2009**, *25*, 10435–10438.
(28) Shirley, D. A. *Phys. Rev. B* **1972**, *5*, 4709–4714.
(29) Shon, Y. S.; Lee, T. R. *Langmuir* **1999**, *15*, 1136–1140.
(30) Marder, M. P. *Condensed Matter Physics*; Wiley-Interscience Publications: New York, 2000.

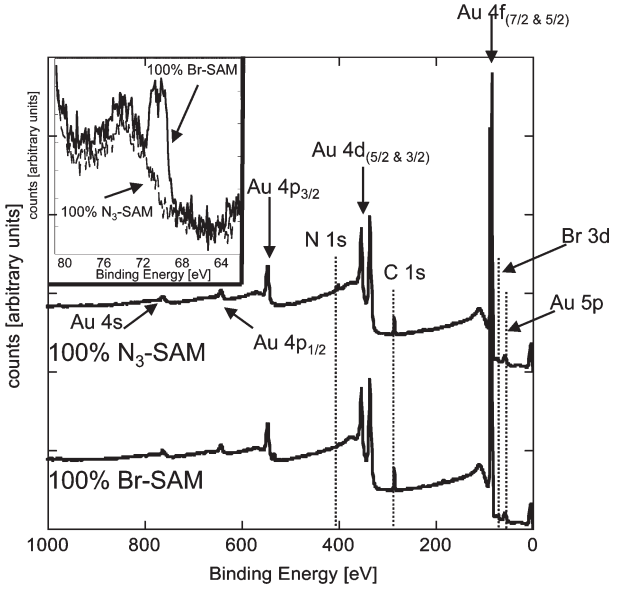

Figure 1. XPS survey spectra of prepared surfaces collected at 1 eV resolution. Bottom spectrum: 100% Br-terminated SAM spectrum with all Au 4f, Au 5p, C 1s, S 2p, O 1s, and Br 3d peaks. Top spectrum: 100% N_3-terminated SAM showed all Au 4f, Au 5p, C 1s, S 2p, O 1s, and N 1s. Nitrogen peaks from the azide were clearly identified, and no Br was detected. The inset shows a high resolution scan on the Br 3d region for the 100% Br-terminated SAM and the 100% N_3-terminated SAM and makes evident the disappearance of the Br signal. Spectra are shown without any baseline correction.

account the change in the index of refraction due to the presence of a single Br atom on the surface. These errors remained small, however, and the trend toward larger surface thicknesses with increasing concentration of bromine termination is clear.

The survey X-ray photoelectron spectrum of a 100% Br-terminated Au surface is shown in Figure 1 (bottom spectrum), where we observed the characteristic peaks for the C and the Au core orbitals. The high resolution scan of the Br 3d binding energy peak at 70 eV is clearly seen in the inset of Figure 1, and its baseline is shaped by the overlap with the weak Cr 3s peak coming from the Cr layer under the Au. The high resolution scan of the S 2p region of this same surface is shown in Figure 2. The presence of the peak at 161.9 eV is the typical shift in binding energy of the sulfur $2p_{3/2}$ orbital due to the Au−S binding interaction,[31,32] and indicates the formation of the self-assembled monolayer through association of the terminal thiol onto the Au surface. The peak at 163 eV was assigned to the spin orbit split S $2p_{1/2}$ orbital which has approximately half of the intensity of the $2p_{3/2}$ peak as expected.[33,34] After 48 h of immersion in the NaN_3 saturated DMF solution, the Br 3d peak disappeared (as shown in the inset of Figure 1) and a peak at approximately 402 eV from the N 1s orbital was observed (Figure 1, top spectrum). A high resolution spectrum of this peak is shown in Figure 3, where we observed the characteristic N_3 doublet at 404.8 and 401.1 eV. The larger intensity peak at 401.1 eV results from the two outer nitrogen atoms of the azide functional group, and the smaller peak at 404.8 eV is characteristic of the electron poor middle nitrogen.[35] The small

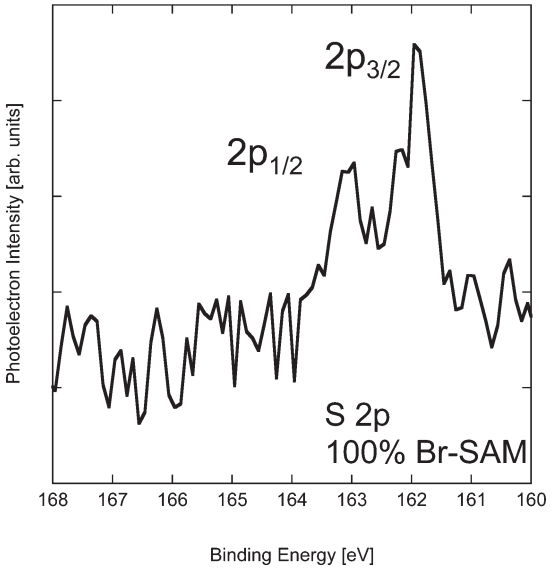

Figure 2. XP spectrum of the S 2p region of a 100% N_3-terminated SAM collected with a resolution of 0.1 eV. The S $2p_{3/2}$ orbital peak was found at 161.9 eV, which was a typical signature for the S binding energy shift due to the Au−S binding interaction. The peak at 163 eV was assigned to the spin orbit split S $2p_{1/2}$ orbital which was approximately half of the intensity of the $2p_{3/2}$. Data is shown without any background correction.

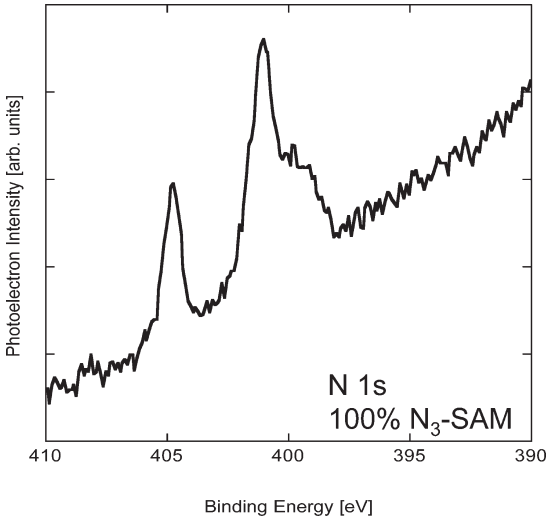

Figure 3. XP spectrum of the N 1s region of a 100% N_3-terminated SAM collected with a resolution of 0.1 eV. Peaks measured at 404.8 and 401.1 eV were characteristic of the azide functional group. Data is shown without any background correction. The small shoulder below 400 eV is photooxidized azide accumulated during the long time necessary to collect the high resolution data.

shoulder below 400 eV is photooxidized azide accumulated during the long time necessary to collect the high resolution data.[36]

Photoelectron spectra were analyzed to determine the extent of surface functionalization of the Br- and N_3-terminated alkane thiols. Figure 4 shows the percentage of surface bromine atoms as a function of the concentration of BrUDT in the thiol solution, and the percentage of nitrogen atoms on surfaces derived from those Br-terminated surfaces. As expected, we observed significantly more nitrogen on each surface than bromine, consistent

(31) Laibinis, P. E.; Whitesides, G. M.; Allara, D. L.; Tao, Y. T.; Parikh, A. N.; Nuzzo, R. G. *J. Am. Chem. Soc.* **1991**, *113*, 7152–7167.
(32) Zhang, S.; Jamison, A. C.; Schwartz, D. K.; Lee, T. R. *Langmuir* **2008**, *24*, 10204–10208.
(33) Laiho, T.; Leiro, J. A.; Lukkari, J. *Appl. Surf. Sci.* **2003**, *212*, 525–529.
(34) Okawa, H.; Wada, T.; Sasabe, H.; Kajikawa, K.; Seki, K.; Ouchi, Y. *Jpn. J. Appl. Phys.* **2000**, *39*, 252–255.
(35) Wollman, E. W.; Kang, D.; Frisbie, C. D.; Lorkovic, I. M.; Wrighton, M. S. *J. Am. Chem. Soc.* **1994**, *116*, 4395–4404.
(36) Wang, P. W.; Hsu, J. C.; Lin, Y. H.; Chen, H. L. *Appl. Surf. Sci.* **2010**, *256*, 4211–4214.

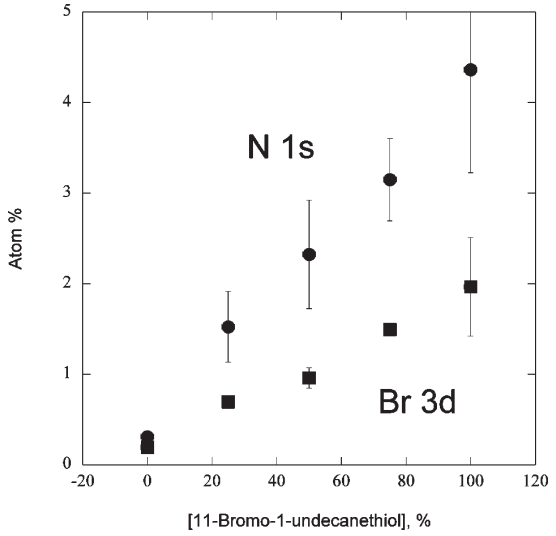

Figure 4. Percentage of Br (squares) and N (circles) atoms on the SAM determined from the ratio of the number of Br or N atoms divided by the sum of all measured atoms and multiplied by 100. For each functionalized surface, the atomic percentage of each element was determined from the average of two different locations. We report the average of five different samples, where error bars represent one standard deviation.

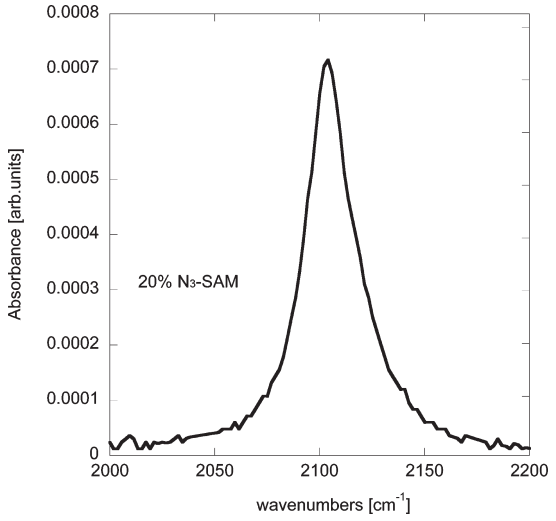

Figure 5. Representative FTIR spectra of the azide asymmetric stretching mode (2103 cm^{-1}) on a 20% N_3-terminated SAM collected with p-polarized light.

with the contribution of three nitrogen atoms from the azide group for each bromine atom. XPS was also used to estimate the relative amount carbon on the surface. Based on the average separation of the thiols on the surface (5 Å)[37] and the size of the surface probed by the XPS spot, we expected to probe approximately 8.61×10^{12} carbon atoms and 2.10×10^{11} bromine atoms on a 25% Br-terminated surface in a survey spectrum, for an expected ratio of 41 carbon atoms for each bromine atom. According to the experimental atomic percentages, we observed a ratio of 48 carbon atoms for each bromine atom. This slight excess of carbon atoms was assigned to adventitious carbon that we were unable to remove from the surface through our cleaning in handling procedures, in agreement with ellipsometry measurements.

(37) Ulman, A.; Eilers, J. E.; Tillman, N. *Langmuir* **1989**, *5*, 1147–1152.

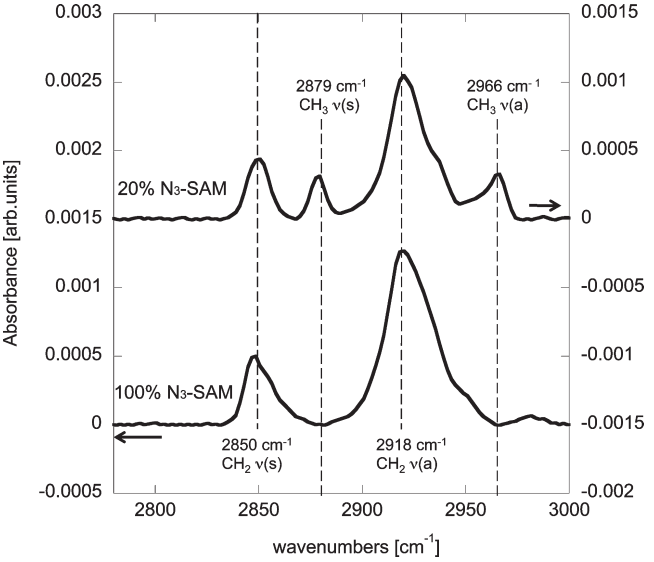

Figure 6. Representative FTIR spectra of the C−H stretching region of a 20% N_3-terminated SAM. The methylene (CH_2−) symmetric and asymmetric stretching modes were measured at 2850 and 2918 cm^{-1}, respectively, while the methyl (CH_3−) symmetric and asymmetric peaks appeared at 2879 and 2966 cm^{-1}, respectively. On a 100% N_3-terminated surface, only the methylene absorptions were measured.

The reactive N_3-terminated surfaces were characterized by GRAS-IR, which provides information on chemical functionality present at the surface and the orientation of the observed functional groups. An azide functional group present on the terminus of a SAM on a relatively flat Au surface should be approximately perpendicular to the plane of the surface. By the selection rules for GRAS-IR, the azide stretching absorption at ~2100 cm^{-1} should therefore interact strongly with p-polarized light.[38,39] Absorption spectra of the azide region derived from a 20% Br-terminated surface (and thus 20% N_3-terminated) in a p-polarized configuration is shown in Figure 5. When illuminating with p-polarized light, we observed a single strong peak at 2103 cm^{-1} corresponding to the azide asymmetric stretching mode. The strong interacting with the p-polarized electric field of the incident light demonstrates that this azide is not parallel to the Au surface. Further characterization of the C−H stretching mode of the alkyl groups methyl (CH_3−) and methylene (CH_2−) on different SAMs is shown in Figure 6. On a 100% N_3-terminated surface, two peaks at 2850 and 2918 cm^{-1} were clearly visible, corresponding to the methylene symmetric and asymmetric peaks, respectively. When the surface coverage of the reactive azide was reduced to a 20% N_3-terminated surface, two additional peaks appeared at 2879 and 2966 cm^{-1}. These were assigned to the symmetric and asymmetric modes of the methyl groups terminating the DT portion of the mixed monolayer SAM. These peaks provide additional characterization on the quality and surface coverage of the self-assembled monolayer and could be used in future work as quality control for calculating the thiol orientation on the SAM.[40]

B. Peptide-Terminated Surfaces. The CD spectrum of αKL(CN-Phe) in 5% (v/v) water in THF demonstrated the characteristic signature of a helical structure with minima in the spectra at 209 and 219 nm (data not shown). This α-helix was reacted with

(38) Lummerstorfer, T.; Hoffmann, H. *Langmuir* **2004**, *20*, 6542–6545.
(39) Crooks, R. M.; Xu, C.; Sun, L.; Hill, S. L.; Ricco, A. J. *Spectroscopy* **1993**, *8*, 28–39.
(40) Nuzzo, R. G.; Dubois, L. H.; Allara, D. L. *J. Am. Chem. Soc.* **1990**, *112*, 558–569.

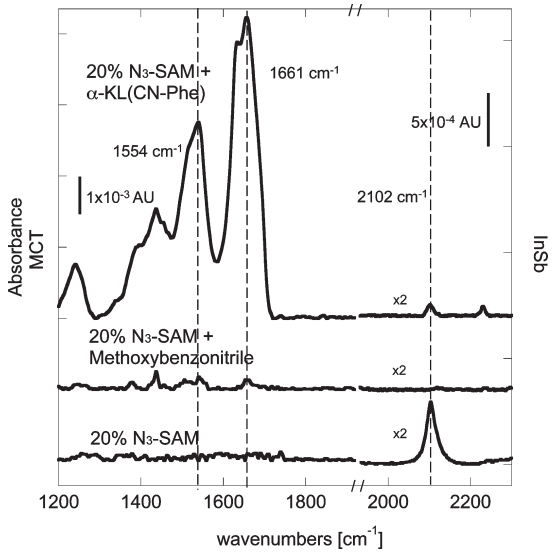

Figure 7. Bottom spectrum: FTIR spectrum of a freshly prepared 20% N_3-terminated surface. Middle spectrum: The product of a 20% N_3-terminated surface reacted with methoxybenzonitrile, resulting in the elimination of the azide stretching mode at 2103 cm^{-1}. Top spectrum: The product of a 20% N_3-terminated surface reacted with αKL(CN-Phe), resulting in substantial elimination of the N_3 stretching mode at 2103 cm^{-1}, the appearance of a peak at 2227 cm^{-1} which we attribute to nitriles on peptides that have bound to the surface through only one tetrazole linker, and the presence of the amide I and II modes at 1658 and 1544 cm^{-1}, respectively. For all spectra, the low energy region from 1200 to 1918 cm^{-1} was measured with a MCT detector (intensities on the left vertical axis), and the high energy region from 1932 to 2300 cm^{-1} was measured with a InSb detector and amplified by a factor of 2 (intensities on the right vertical axis). Scale bars for the intensity of each vertical axis are shown.

20% N_3-terminated surfaces in the presence of 100 mol equiv of DEAD in 5% (v/v) water in THF. After the reaction, the average thickness of the peptide-terminated SAM was 2.7 ± 0.2 nm, determined from ellipsometry. This is approximately 0.7 nm thicker than the 20% N_3-terminated surface, an increase in thickness of about half the diameter of the peptide or about one-sixth of its length. XPS spectra of the peptide-terminated SAMs indicated the presence of the previously seen S 2p doublet located at the same characteristic binding energies for the S−Au interaction listed above. This measurement proves that the SAM is not severely affected after the last reaction and rinsing cycle.

Representative GRAS-IR spectra of these surfaces are shown in Figure 7, compared with the 20% N_3-terminated surface from which they were prepared (bottom spectrum). In these spectra, the region from 1200 to 1918 cm^{-1} was collected with a MCT detector, but from 1932 to 2300 cm^{-1} a InSb detector was used to take advantage of its enhanced sensitivity in this region. No other features were observed from these 20% N_3-terminated surfaces throughout the spectral range shown in Figure 7, and therefore, any other peaks that appear in later measurements are the consequences of further chemical reactions on this azide-terminated surface. These results are summarized in Table 2. To test our reaction conditions, the 20% N_3-terminated surface was also reacted with methoxybenzonitrile, resulting in complete loss of the N_3 peak at 2103 cm^{-1}. No significant features other than the carbon−carbon double bond at 1438 cm^{-1} were observed in the resulting GRAS-IR spectrum (middle spectrum in Figure 7).

The top spectrum in Figure 7 shows a surface that resulted from exposing a 20% N_3-terminated SAM with αKL(CN-Phe) under our reaction conditions. A small but measurable peak at 2103 cm^{-1} was observed, indicating that a small amount of N_3 remained on the surface, even after 24 h of reaction time. As expected, large amide peaks appeared in the low energy region at 1544 and 1658 cm^{-1}, corresponding to the amide II and I modes, respectively. A small peak at 2227 cm^{-1} also appeared on the peptide-terminated surface, attributed to the nitrile stretching mode of the CN-Phe on the peptide.[41] This unreacted nitrile group would be present only if some fraction of the surface-bound peptides had reacted with only one available nitrile group, resulting in the presence of the free, unreacted nitrile group tethered to the surface through the chemically bound peptide. Finally, we observed a small C−O stretch at 1240 cm^{-1} and an aromatic C=C stretch at 1438 cm^{-1} that overlaps with C−H aromatic in plane bending from the phenyl ring.[42] Because it is possible that a peptide that was not chemically bound to the surface could remain absorbed on the SAM after our reaction, we performed a control experiment in which a 100% DT-composed surface (i.e., without the reactive azide group) was exposed to the peptide under our reaction conditions and then washed thoroughly according to the procedure described above. No amide or nitrile peaks were observed on these control surfaces, suggesting that there is no detectable physical absorption of the peptide on the SAM in the absence of a chemical bond being formed between the peptide and the surface, and that it is only in the presence of DEAD, the N_3-terminated SAM, and the nitrile group, simultaneously, that the surface reacts to form the tetrazole linker.

The reaction yield was determined from GRAS-IR spectra by first evaluating how much azide was lost under the reaction conditions without a nitrile reagent. The amount of azide lost in this reaction was attributed to damage to the SAM, not tetrazole formation. To monitor this damage of the azide on the SAM, we measured the intensity of the azide peak stretching mode at 2103 cm^{-1} after exposing the sample to 5% (v/v) water in THF and 10 μmol DEAD. After the reaction, these controls had the same spectral features as the original 20% N_3-terminated SAM but a weaker azide signal. The loss in the azide intensity was between 50 to 53% for all control samples. All reaction yields reported for reactions solutions with cyanides were normalized with respect to this control. The good reproducibility of the loss of the azide peak of the control samples was necessary for small reaction yield errors. When αKL(CN-Phe) was reacted with the surface, the extent of the reaction appeared directly dependent on the DEAD concentration in the reaction solution. As seen in Table 2, with 177 nmol of peptide (354 nmol of CN), 5 mol equiv of DEAD resulted in a reaction yield of 37%, while 50 mol equiv of DEAD doubled the reaction yield to 80%.

The relative intensity of the amide I and II peaks measured by GRAS-IR can be used to assess the relative orientation of the peptide on the surface according to eq 2:

$$D = K\frac{2[1/2(3\cos^2\theta - 1)][1/2(3\cos^2\theta_I - 1)] + 1}{2[1/2(3\cos^2\theta - 1)][1/2(3\cos^2\theta_{II} - 1)] + 1} \qquad (2)$$

where D is the calculated ratio between the integrated areas of the amide I and the amide II peaks on the SAM, θ_I is the angle between the amide I mode and the helix backbone, θ_{II} is the angle between the amide II mode and the helix backbone,[43] K is the

(41) Babkov, L. M.; Gnatyuk, I. I.; Trukhachev, S. V. *J. Mol. Struct.* **2005**, *744−747*, 425–432.
(42) Diaz-Fleming, G.; Golsio, I.; Aracena, A.; Celis, F.; Vera, L.; Koch, R.; Campos-Vallette, M. *Spectrochim. Acta, Part A* **2008**, *71*, 1074–1079.
(43) Miura, Y.; Kimura, S.; Imanishi, Y.; Umemura, J. *Langmuir* **1998**, *14*, 6935–6940.

Table 2. Percentage of N_3-Terminated Surface, Reagent Type and Amount, Molar Equivalents of DEAD per Reactive Nitrile (CN) for Each Reaction Condition, Huisgen Cycloaddition Percent Yield, and Indication of the Presence and Magnitude of Amide Peaks near 1550 and 1650 cm^{-1} on the Sample Surface

% N_3 on SAM	reagent	reagent nmol	DEAD CN equiv	reaction yield %	amide peaks present
20	methoxybenzonitrile	1000	50	98	no
20	toluene nitrile	1000	50	80	no
20	α-KL(CN-Phe)	177	5	37	small
20	α-KL(CN-Phe)	177	50	80	large
controls					
20	methoxybenzonitrile	1000	0	0	no
0	α-KL(CN-Phe)	177	75	0	no
20	none	0	[DEAD] = 670 μM	0	no

proportionality constant determined from the ratio of the integrated areas of amide II to amide I measured in a solution of randomly oriented αKL(CN-Phe), and θ is the angle between the surface normal and the helical axis.[44] The amide angles θ_I and θ_{II} were calculated from a peptide model that was made with Avogadro 1.00, an open-source molecular builder and visualization tool.[45] The energy of the helical structure was minimized using the MMFF94 force field, using a steepest descent algorithm in 500 steps with a convergence precision of seven significant figures. After energy minimization, the atomic coordinates where manipulated in Mathematica 7 to fit a line through the peptide backbone and another through the carbonyl atom pair for the amide I direction and through the N−C atom pair for the amide II direction.[46] The angle between the peptide backbone and the carbonyl was assigned to θ_I, which was determined to be $35 \pm 8°$, while the angle between the N−C bond was assigned to θ_{II}, which was determined to be $63 \pm 10°$; the reported error is the standard deviation of all amide bonds in the helix. To measure the proportionality constant K, we collected the FTIR spectrum of the peptide in a solution containing 2 mM αKL(CN-Phe) in 5% (v/v) water in THF inside a liquid cell composed of sapphire windows separated by a path length of 125 μm, and compared this spectrum against a background of the identical solution without peptide. The ratio of the integrated areas under the amide II to amide I peaks was found to be 2.06, which was assigned to K. With all the above measured parameters, eq 2 was used to determine a value of $\theta = 53 \pm 11°$, where the error is given by the standard deviation of the five measured samples. This angle range indicates that, on average, the peptide was randomly oriented on top of the surface.

Discussion

To generate biomimetic surfaces, our goal is to prepare surfaces functionalized with peptides that are bound to the surface with strict control over their secondary structure, orientation, and concentration. Our strategy to fulfill this goal is to link peptides to well-characterized surfaces through at least two covalent bonds, to provide additional integrity and stabilization of the desired peptide structure. In the work described here, generating mixed monolayers of a reactive azide-terminated alkane thiol and an inert thiol at specific surface coverage of the reactive functionality allows us to direct subsequent surface chemistry with nitrile-containing peptides introduced to the surface. To generate the azide-terminated surfaces, we prepared mixed monolayers of BrUDT in DT at varying concentration of BrUDT in the initial monolayer solution. Ellipsometry and XPS verified that the surface coverage of bromine termination on the surface increases in an expected manner as the concentration of BrUDT in DT increased in the SAM preparation solution. A surface that is 20% terminated in the reactive azide functional group, considering the alkyl spacing of 5 Å, therefore places the azide groups approximately 25 Å from each other on the completed surface, provided that these functional groups are homogeneously distributed on the surface. While with a mixture of a fraction of BrUDT in DT it is likely that this will be the case, further work in our laboratory is focused on determining the spatial distribution of functional groups across the surface, for all terminated surfaces discussed here, and will be reported in later publications. This control is important for subsequent functionalization of the surface.

Our selection of a peptide containing a terminal nitrile group to react with the surface-bound peptide has required optimization of the Huisgen cycloaddition reaction conditions. We have employed and modified reaction conditions that were shown to be useful in the formation of hindered tetrazoles[47] and have worked well under our test conditions with the molecules methoxybenxonitrile and methylbenzonitrile. The disappearance of the strong azide asymmetric stretching mode at 2103 cm^{-1}, which does not occur under our control conditions, indicates that the azide had reacted with the terminal nitrile, which then remains bound to the surface. Furthermore, the C=C double bonds from the phenyl ring of these molecules were detected on the surface after the reaction at 1438 cm^{-1}. Upon addition of the nitrile-containing peptide in the presence of a large excess of DEAD, we measured the disappearance of the azide group, which, by comparing to the control surfaces, we attribute to the reaction between the nitrile and surface-bound azide.

The interactions between the αKL(CN-Phe) peptide and various surfaces have been extensively studied by sum frequency generation,[48] time-of-flight secondary ion mass spectrometry,[49] and atomic force microscopy.[50] This amphiphilic peptide was initially designed to have all hydrophobic leucine side chains pointing to the opposite direction of the hydrophilic lysine side chains and its adhesion properties onto hydrophobic and hydrophilic surfaces have been studied in water.[51] The cyanophenylalanine unnatural amino acids were positioned on αKL(CN-Phe) in a sequence designed to present the nitrile group on the same side of the structured α-helix approximately 25 Å apart. The reaction

(44) Uzarski, J. R.; Tannous, A.; Morris, J. R.; Mello, C. M. *Colloids Surf., B* **2008**, *67*, 157–165.
(45) Ali, S.; Banck, M.; Braithwaite, R.; Bunt, J.; Curtis, D.; Fox, N.; Hanwell, M.; Hutchison, G.; Benoit, J.; Lonie, D.; Mantha, J.; Margraf, T.; Niehaus, C.; Ochsenreither, S.; Vandermeersch, T.; http://avogadro.openmolecules.net, 2010.
(46) Parson, W. W. *Modern Optical Spectroscopy*; Springer: New York, 2007.
(47) Duncia, J. V.; Pierce, M. E.; Santella, J. B. *J. Org. Chem.* **1991**, *56*, 2395–2400.
(48) Weidner, T.; Apte, J. S.; Gamble, L. J.; Castner, D. G. *Langmuir* **2009**, *26*, 3433–3440.
(49) Apte, J. S.; Collier, G.; Latour, R. A.; Gamble, L. J.; Castner, D. G. *Langmuir* **2010**, *26*, 3423–3432.
(50) Mermut, O.; Phillips, D. C.; York, R. L.; McCrea, K. R.; Ward, R. S.; Somorjai, G. A. *J. Am. Chem. Soc.* **2006**, *128*, 3598–3607.
(51) DeGrado, W. F.; Lear, J. D. *J. Am. Chem. Soc.* **1985**, *107*, 7684–7689.

of one of the nitrile groups to form the tetrazole linker will then tether the entire peptide, including the second peptide nitrile group to the surface. This nitrile will either to remain unreacted or react with an additional azide within approximately 25 Å. If it reacts with a nearby azide, the peptide will then be chemically bound to the surface at two locations in a manner that allows the α-helical structure of the peptide to be maintained and provides some structural rigidity. However, the observation of a small remaining azide peak at 2103 cm^{-1}, as well as the addition of a small peak at 2227 cm^{-1}, attributed to the nitrile group on CN-Phe, indicate that the final functionalized surface contains some peptides that have not reacted with azide. Our control experiments confirm that no peptide remains absorbed on the surface in the absence of a chemical bond; therefore, this nitrile peak must be from surface-bound peptides that have only reacted at one of the available nitrile groups. Current work in our laboratory is focused on tuning the concentration of the reactive azide on the N_3-terminated surface and our reaction conditions for optimum reactivity with the peptide to result in peptides that have reacted all available nitrile groups.

Circular dichoric spectroscopy demonstrated that the αKL-(CN-Phe) peptide maintained its α-helical structure in our reaction conditions, 5% (v/v) water in THF. This implies that the separation of the two cyanides on the peptide remains optimum for the average separation of the azides on the surface at the moment of reaction and that we expect the peptide to be tethered to the surface at two different points. However, at the end of the reaction, the surface was washed in copious amounts of organic solvent and water and then thoroughly dried. It is therefore not possible to predict the secondary structure of the peptide under these extensively perturbed conditions. To quantify this, we have studied the structure of the surface-bound peptide using the surface polarization of the amide I and II modes.[52] These two vibrational modes absorb p-polarized light with different intensities, which can be measured to estimate the structure and orientation of the peptide. When the peptide backbone is arranged in a single and ideal helical structure, these amide peaks have an intensity ratio that is intrinsic to the helical nature of the secondary structure and act as a spectroscopic fingerprint. Changes in the secondary structure after the peptide is bound to the surface can therefore be monitored by measuring this ratio on the SAM surface. When an ensemble of ideal helical structures is measured, the ratio of the two amide peaks changes only as a function of the relative orientation of the helixes with respect to each other. When the ensemble of αKL(CN-Phe) is chemically bonded to a surface at two points, the relative orientation of the peptides is no longer random but is directed by the structure of the surface, in this case a nominally flat monolayer. The orientation of these peptides on the surface was measured by quantifying the angle, θ, of the helix backbone with respect to the surface normal. This angle was calculated using eq 2 by assuming that the structures of individual peptides in the ensemble were not significantly perturbed from the original helix structure and that the angle of the amide I and II vibrational modes, θ_I and θ_{II}, could be determined from a model of the α-helical structures. These two amide angles could of course change depending on the extent of deformation of the helical structure; computational modeling of these peptides under our particular reaction conditions is necessary for improving our approximation. This is analysis could also be affected by the extent of chemical inhomogeneity of the surface, either from aggregation of the reactive N_3-terminated alkyls or from extensive disruption of the alkyl monolayer caused by the peptide-termination chemistry. Chemical analysis of these and other questions is currently underway in our laboratory and will be the focus of future publications.

Even given the inherent limitations of the relationship between the surface-bound structure and the solution structure, we still are able to form some qualitative conclusions about the structure of the peptide-functionalized surface. We determined the average orientation of the helix with respect to the surface normal, θ, to be $53 \pm 11°$. Based on all of the evidence from infrared spectroscopy of the surface, it is likely that this measurement is a convolution of helices bound by one and two chemical bonds, both maintaining and losing the designed α-helical structure. This represents a surface that, while containing biologically compatible amino acid functional groups, does not organize those groups in a structured and predictable manner. Furthermore, this analysis could be disrupted if the surface has an inhomogeneous distribution of reactive functional groups (discussed above) or there is extensive disruption to the alkyl monolayer during the peptide functionalization reaction. Therefore, these two aspects in particular must be carefully studied in order for this strategy to be fulfilled. We believe that this goal can be achieved by optimization of the concentration of surface-bound azides, the distance between reactive nitrile groups on the peptide, and our reaction conditions. Further work on all of these fronts is underway in our laboratory.

In conclusion, we have synthesized and characterized peptide-functionalized gold surfaces that connect the highly organized structure of a thiol SAM on gold with biologically relevant structural elements such as an α-helix. While this peptide maintains its α-helical character under our reaction conditions, the resulting surface results in peptides that are randomly oriented and/or unstructured. Ongoing work focuses on a number of facets, including preventing loss of the azide functional group during the reaction, tuning the surface coverage and reaction conditions to result in all surface-bound peptides reacting through both nitrile groups, exploring the amino acid sequence that will result in predicted structure such as a α-helix, and expanding our structured peptides to include β-sheet like peptides, to compare the difference in surface chemical functionalization of different peptide structures under similar reaction conditions. We are also extending these studies to surface spectroscopic methods that can be collected in situ, to determine the exact consequences of dehydrating the surface after peptide functionalization.

Acknowledgment. This work was funded by the Army Research Office (Grant No. W911NF-10-1-0280). We thank Ms. Michelle Gadush at the Institute for Cell and Molecular Biology at The University of Texas at Austin for peptide synthesis, the Texas Materials Institute for their support of the clean room and ellipsometry equipment, and the National Science Foundation for funding the Kratos X-ray photoelectron spectrometer (Grant No. 0618242). L.J.W. holds a Career Award at the Scientific Interface from the Burroughs Wellcome Fund.

Note Added after ASAP Publication. This article was published ASAP on November 18, 2010. The title of the manuscript has been modified. The correct version was published on November 24, 2010.

(52) Fujita, K.; Bunjes, N.; Nakajima, K.; Hara, M.; Sasabe, H.; Knoll, W. *Langmuir* **1998**, *14*, 6167–6172.